Available online at www.sciencedirect.com

SCIENCE DIRECT®

Magnetic Resonance Imaging 23 (2005) 679–684

MAGNETIC RESONANCE IMAGING

Renal-related perinephric fluid collections: MRI findings

N. Cem Balci[a,*], Elif Akun[b], Mehmet Erturk[c], Sezer Saglam[d], Nagihan Inan[a], Yesim Balci[e]

[a]Department of Radiology, SLU, St. Louis, MO 63110, USA
[b]Department of Internal Medicine, Kadir Has University, Istanbul 36600, Turkey
[c]Department of Radiology, Sisli Etfal Hospital, Istanbul 64460, Turkey
[d]Department of Medical Oncology, Istanbul Medical Faculty, Istanbul 29980, Turkey
[e]Department of Anesthesiology, Istinye Hospital, Istanbul 36460, Turkey

Received 7 October 2004; accepted 11 April 2005

Abstract

We retrospectively reviewed MR studies on 10 patients with renal-related perinephric fluid collections who underwent MRI in three institutions between January 2001 and August 2004. All patients underwent MRI of the abdomen and T1-weighted, T2-weighted and serial contrast-enhanced images, including delayed-phase contrast-enhanced images 10–12 min after contrast injection, were obtained. Perinephric fluid collections in 5 patients revealed MRI findings of simple fluid content (i.e., hypointense on T1-weighted images and hyperintense on T2-weighted images). In another 5 patients, a complex perinephric fluid content (i.e., mixed hyper/hypointense on T1-weighted images and mixed hypo/hyperintense on T2-weighted images compatible with blood breakdown products and pus) was observed. In 5 patients, contrast extravasation on late-phase images that was compatible with urine leak was demonstrated. Our results suggest that MRI may determine the content of perinephric fluid collections on noncontrast T1-weighted and T2-weighted images and that contrast extravasation on late-phase images is associated with urine extravasation from renal collecting systems.

Keywords: Kidney; Hemorrhage; Urinoma; Urine extravasation

1. Introduction

Retroperitoneal fluid collections in the perinephric spaces are not uncommon. They may contain pus, urine, blood and lymph or transudate fluid resulting from kidney-related pathologies or from retroperitoneal structures [1]. Fluid collections that have communication with the renal parenchyma and collecting system need to be depicted immediately because of the insidious accumulation of renal-related fluid [1–3]. CT has been the method of choice for the assessment of retroperitoneal fluid collections, with a sensitivity of 100% and specificity of 77% [3,4]. However, MRI findings of retroperitoneal fluid collections have also been reported [3]. MRI can evaluate the nature of fluid collections in the abdomen. Differentiation between transudate, abscess and hemorrhage is possible with MRI [3]. It is sensitive for the specific determination of the age of a hemorrhage [5–8]. Nevertheless, MRI findings of renal-related retroperitoneal fluid collections have not been investigated in larger series. The aim of this study is to describe the spectrum of MRI findings of renal-related perinephric fluid collections.

2. Materials and methods

Over a period of 3 years, we observed 10 patients (6 males and 4 females; age range, 6–78 years) with retroperitoneal fluid collection in the perinephric spaces on MRI. All these patients were referred to MRI after an initial abdominal ultrasound examination that detected perinephric fluid collection. MRI was performed to further investigate the cause of the perirenal fluid collections: 2 patients were under follow-up of known hydronephrosis, 2 had a recent history of blunt abdominal trauma and 4 underwent MRI to rule out spontaneous fornix and/or ureter rupture. One patient underwent fine-needle biopsy of a renal cystic mass. Another patient was undergoing an anticoagulation therapy and had decreased INR levels. All patients underwent surgical intervention to clean up the perinephric fluid.

* Corresponding author.
E-mail address: nc.balci@excite.com (N.C. Balci).

0730-725X/$ – see front matter © 2005 Elsevier Inc. All rights reserved.
doi:10.1016/j.mri.2005.04.003

All MR studies were retrospectively reviewed by two investigators (N.C.B. and M.E.). The location, nature and source of the fluid and its association with renal pathologies were assessed in each patient. The signal intensities of the fluid collections were compared with the psoas muscle and considered hypointense if the signal was lower and hyperintense if the signal was higher than the signal of the psoas muscle.

All patients underwent MR examination on a 1.5-T scanner in three institutions [Sonata ($n=5$) and Vision ($n=1$), Siemens Medical Systems, Erlangen, Germany; Signa Horizon ($n=1$), GE Medical Systems, Milwaukee, WI, USA; Intera ($n=3$), Philips Medical Systems, Best, the Netherlands]. Axial T1-weighted breath-hold spoiled gradient echo (SGE) images (TR/TE/FA, 150–180/4.2/80 in phase and 150–180/2.3/80 out of phase) were obtained from all patients; axial T1-weighted breath-hold SGE images with spectral fat suppression (TR/TE/FA, 150–180/4.2/80) were obtained from 7. T2-weighted images included T2-weighted half-Fourier single-shot fast spin echo images obtained with and without fat suppression in the axial plane (TR/TE, ∞/90) and without fat suppression in the coronal plane ($n=6$), respiratory-gated T2-weighted fast spin echo images (TR/TE/ETL, 4800/90/8) with fat suppression in the axial plane ($n=1$) and T2-weighted balanced fast field echo (TR/TE/FA, 4.8/2.1/70) images in both axial and coronal planes ($n=8$). Gadolinium chelate (Magnevist, Schering, Berlin, Germany) was administered at a dose of 0.1 mmol/kg as a 5-s hand-injected bolus followed by a rapid flush of 10 ml of normal saline. In-phase SGE (TR/TE/FA, 150–180/4.2/80) images were acquired immediately after contrast administration (arterial phase) and at 45 and 90 s (intermediate phase) and at 7–10 min (delayed phase) after completion of the normal saline flush. Late contrast images were obtained with the use of SGE sequence (TR/TE/FA, 150–180/4.2/80) with ($n=7$) and without ($n=3$) fat suppression in coronal and axial planes in all patients.

3. Results

The perinephric fluid collections were confined in the perirenal space in three patients. In seven patients, perinephric fluid collections were located in more than one compartment: perirenal and anterior pararenal spaces ($n=4$); perirenal and posterior pararenal spaces ($n=2$); and all of the perirenal anterior and posterior pararenal spaces ($n=1$).

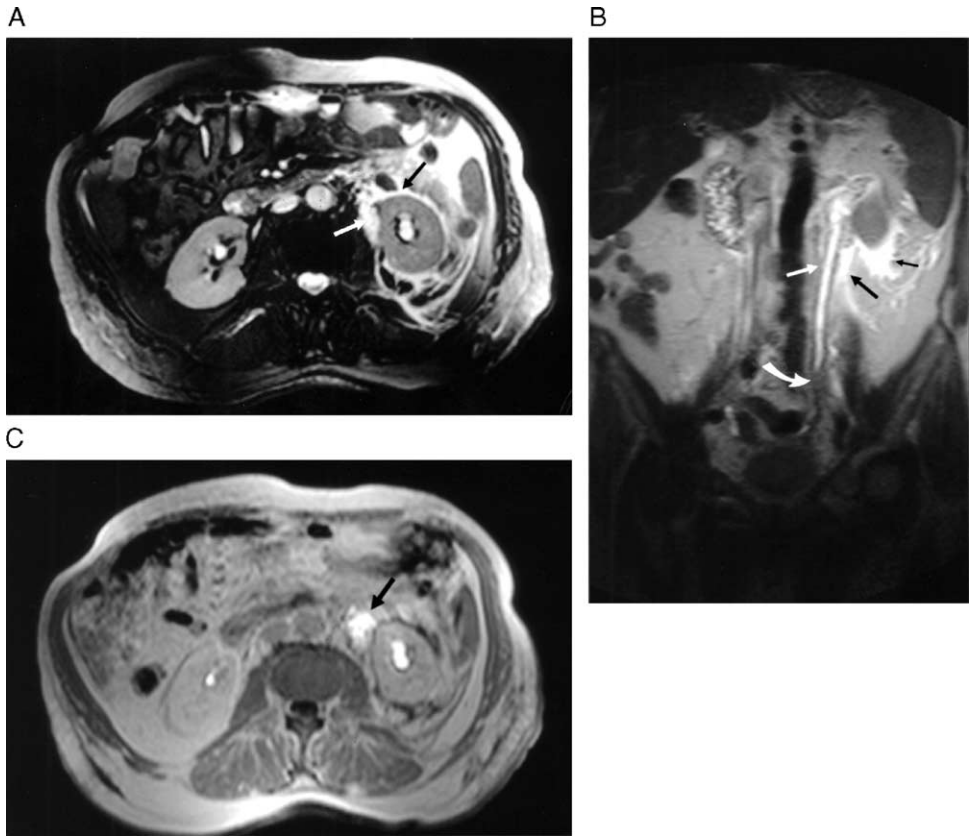

Fig. 1. MRI of a 32-year-old patient who presented with retroperitoneal fibrosis with complicated hydronephrosis on follow-up. (A) Axial T2-weighted balanced fast field echo image (TR/TE/FA, 4.8/2.1/70) showing hyperintense perinephric fluid collection (arrows). (B and C) Coronal T2-weighted half-Fourier single-shot fast spin echo images showing dilated ureter (white straight arrow, B) and the causing retroperitoneal fibrosis (curved arrow, B). The retroperitoneal perinephric fluid collection is also visible (black straight arrows, B). (C) Late contrast-enhanced T1-weighted SGE image (TR/TE/FA, 150/4.2/80) showing retroperitoneal contrast extravasation (arrow).

Perirenal contrast extravasation was observed in five patients. In four of these patients, a simple fluid content was observed (i.e., hypointense on T1-weighted images and hyperintense on T2-weighted images; Fig. 1). In one patient with a history of blunt abdominal trauma, the perirenal fluid revealed a mixed signal (hypo/hyperintense) on both T1-weighted and T2-weighted images that was compatible with urine–blood mixture in the fluid (Fig. 2).

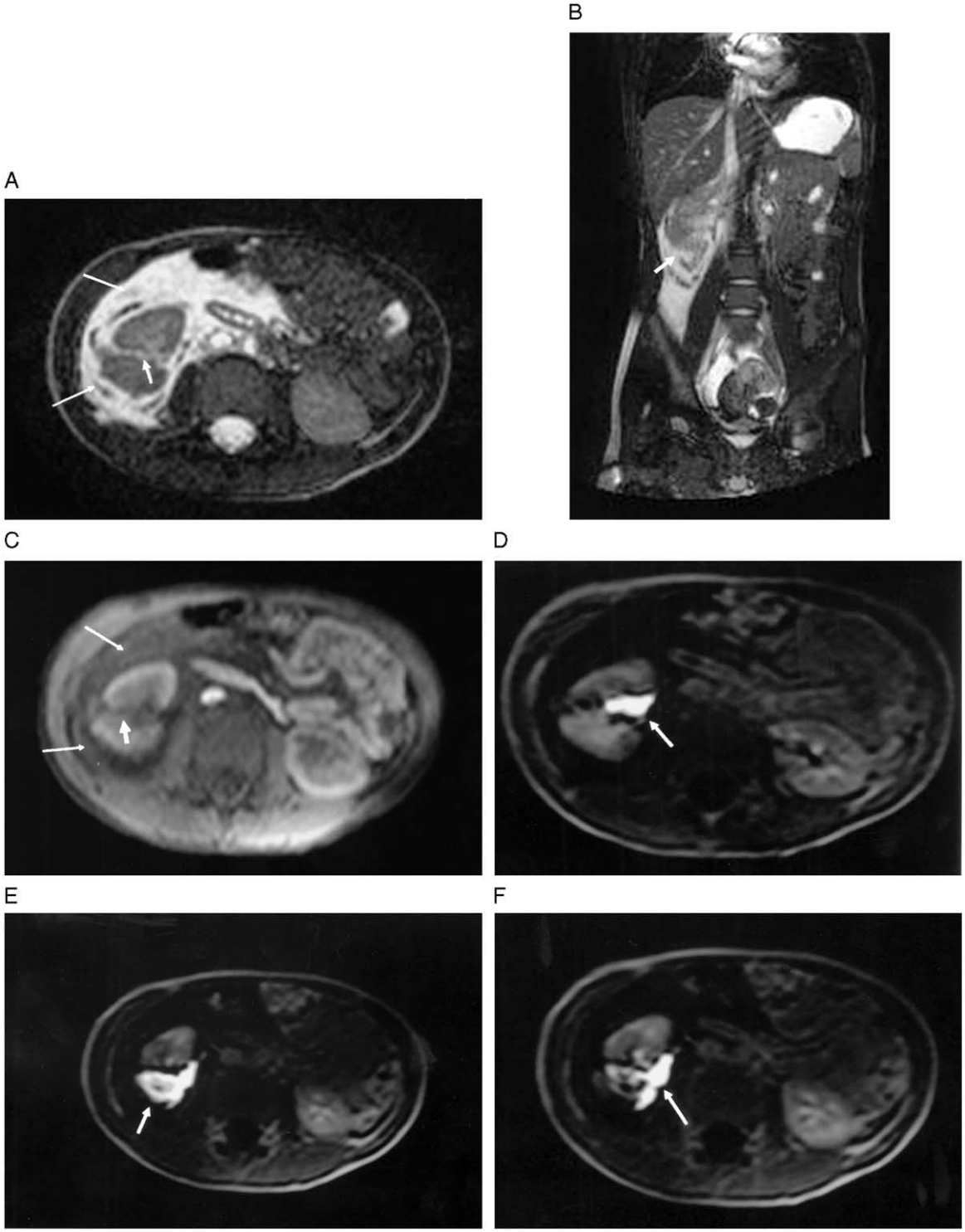

Fig. 2. Renal laceration secondary to acute blunt abdominal trauma. Axial (A) and coronal (B) T2-weighted balanced fast field echo images (TR/TE/FA, 4.8/2.1/70) showing perinephric fluid with a hyper/hypointense mixed signal (thin long arrows, A) and the laceration site (thick arrows, A and B). (C) T1-weighted fat-saturated SGE image (TR/TE/FA, 167/4.2/80) showing perinephric fluid with a hyper/hypointense mixed signal compatible with a mixed acute and subacute hemorrhage (arrows, C). (D–F) Late enhanced T1-weighted SGE images (TR/TE/FA, 156/4.2/80) demonstrating contrast extravasation (arrows).

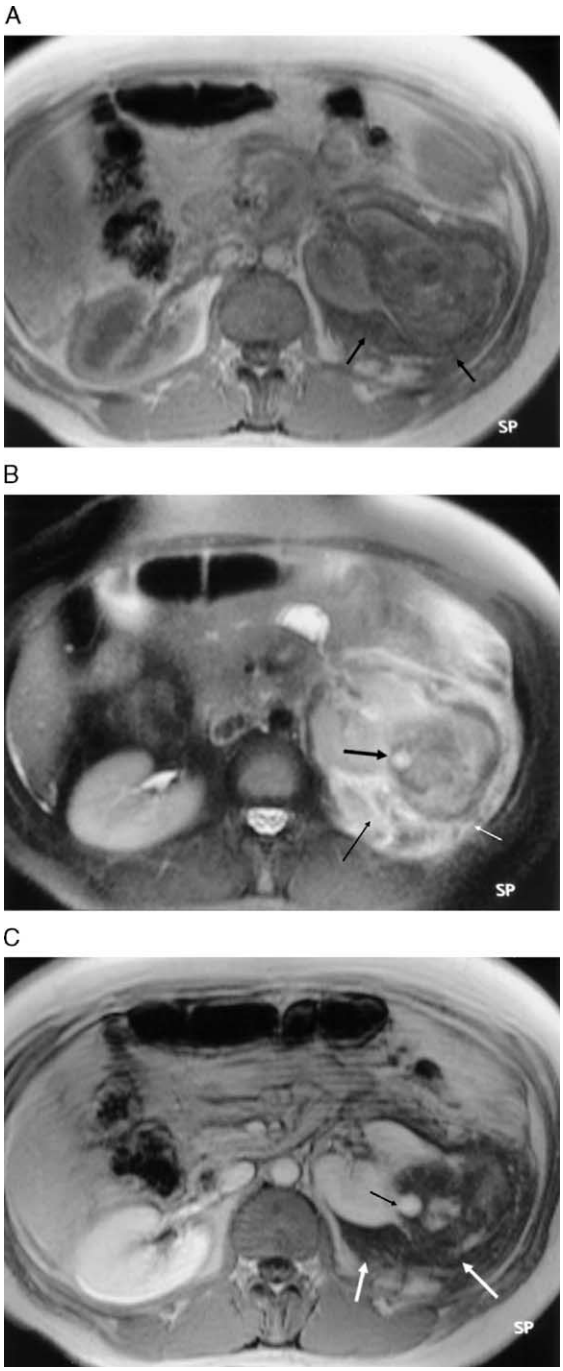

Fig. 3. Perinephric fluid extravasation as a result of the biopsy of cystic renal cell carcinoma. (A) Axial T1-weighted SGE image (TR/TE/FA, 165/4.2/80) revealing perinephric fluid collection in the perirenal space with a hyper/hypointense mixed signal (arrows). (B) Axial T2-weighted fat-saturated T2-weighted half-Fourier single-shot fast spin echo images (TR/TE, ∞/90) demonstrating perinephric fluid collection with a hypo/hyperintense mixed signal (thin arrows) and a hyperintense mural nodule within the cystic mass (thick black arrow). (C) Delayed postcontrast axial T1-weighted SGE image (TR/TE/FA, 150–180/4.2/80) showing that the perinephric fluid collection is hypointense relative to the kidney and that the mural nodule reveals intense enhancement (thin black arrow).

No contrast extravasation was observed in the other five patients. In four of these patients, the perirenal fluid revealed a mixed signal on both T1-weighted and T2-weighted images that was compatible with blood, pus and mixture of blood and pus (Figs. 3 and 4). One patient with confined urinoma presented a simple fluid content (i.e., hypointense on T1-weighted images and hyperintense on T2-weighted images).

4. Discussion

Perinephric spaces are considered as retroperitoneal anatomical spaces that consist of perirenal and anterior and posterior pararenal spaces. Perinephric spaces can harbor fluid collections that are related to organ pathologies within these anatomical spaces or that may originate from the adjacent intraperitoneal or retroperitoneal organs [9]. Kidneys, including the renal collecting system, are highly vascular organs; they are the major fluid gateway of the body. Fluid collections that are associated with renal pathologies contain urine, blood, pus or transudate [1]. Etiologies of renal-related fluid collections include renal trauma, spontaneous calyceal rupture, spontaneous rupture of existing renal pathologies such as cysts, hydronephrosis and mass lesions [2,8–12]. Renal vascular pathologies may rarely cause hematoma in the perinephric spaces [13].

The causes of renal-related retroperitoneal hemorrhage are renal trauma and spontaneous or posttraumatic bleeding of existing renal pathologies. Nontraumatic renal hematoma occurs secondary to spontaneous rupture of renal cell carcinomas, angiomyolipomas or hemorrhagic renal cysts. Blood dyscrasia and anticoagulation therapy are predisposing conditions for spontaneous renal hematomas [6]. In our series, we observed one patient with spontaneous renal cyst bleeding as a complication of anticoagulation therapy. This is not an uncommon complication of anticoagulation therapy and requires early diagnosis for the cessation of the therapy on time [2,11]. MRI findings of retroperitoneal hematoma have been described according to different ages of hemorrhage. It has the same MR signal characteristics as do other intraabdominal hematomas [11]. Abdominal hematomas in the acute stage are hypointense on T1-weighted and T2-weighted images. Hypointensity on T1-weighted and T2-weighted images determines the acute age of a hematoma. In the acute stage, blood erythrocytes contain deoxyhemoglobin, which is paramagnetic and has strong T2-shortening effects [3,4]. In the subacute stage, intracellular methemoglobin is responsible for the hyperintense signal on T1-weighted images and the hypointense signal on T2-weighted images [3,4]. The mixed signal intensity in our cases may have been related to (a) hemorrhages with varying acute and subacute ages of blood breakdown products (i.e., acute bleeding on subacute hemorrhage) and (b) mixture of urine with blood breakdown products.

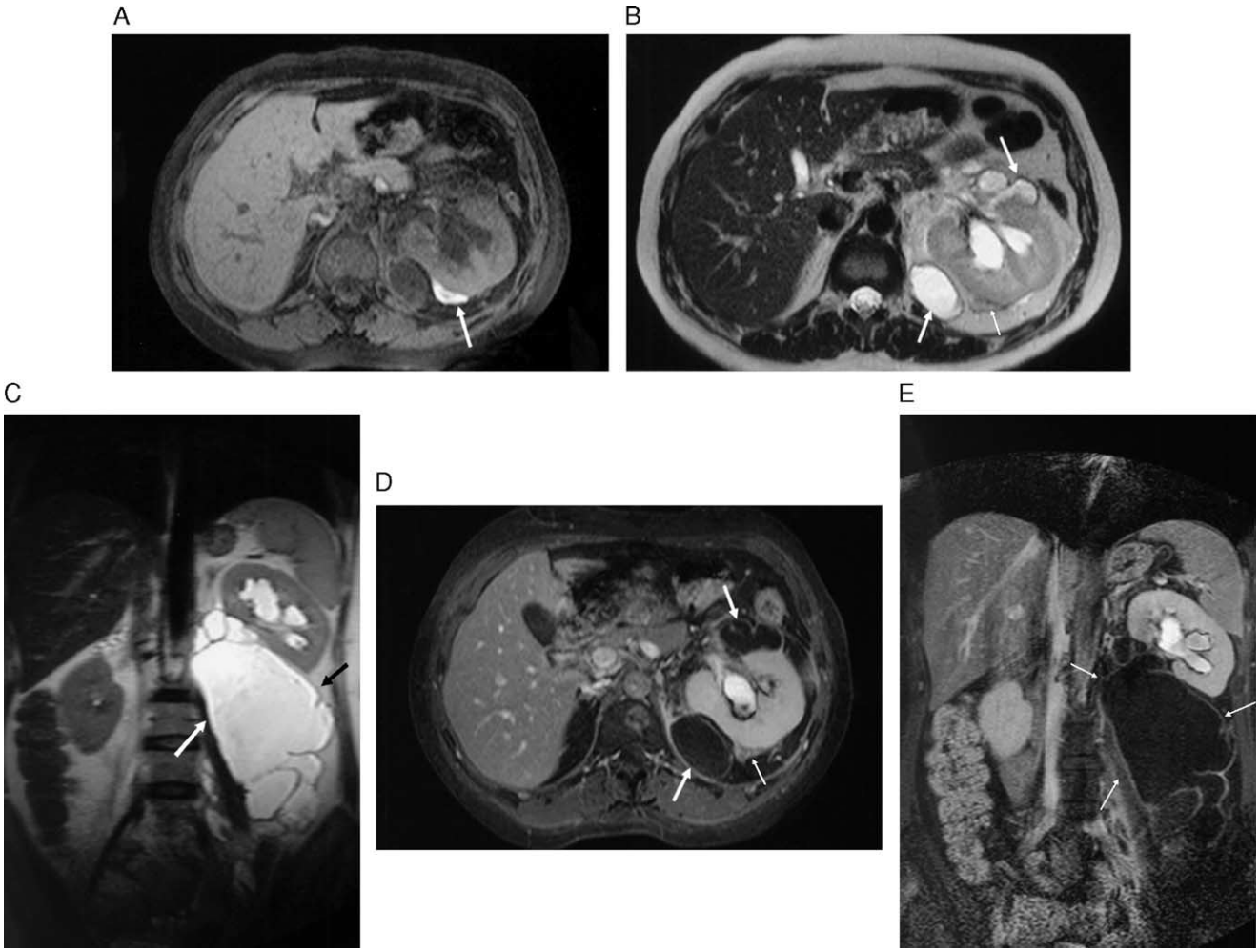

Fig. 4. Urinoma formation secondary to traumatic perirenal rupture of a long-standing hydronephrosis. (A) Axial T1-weighted fat-saturated SGE image (TR/TE/FA, 158/4.2/80) revealing a thin subcapsular subacute hematoma secondary to trauma (arrow). T2-weighted half-Fourier single-shot fast spin echo images in axial (B) and coronal (C) planes (TR/TE, ∞/90) revealing hyperintense fluid collections in the perirenal space (thick arrows) with a thin rim. On axial T2-weighted half-Fourier single-shot fast spin echo image, the subcapsular hematoma is hypointense (thin arrow, B). On late postcontrast T1-weighted fat-saturated SGE images (TR/TE/FA, 178/4.2/80) in axial (D) and coronal (E) planes, the urinoma has a hypointense content with rim enhancement (arrows, D and E); the subcapsular hematoma is marked with a thin arrow on the axial late contrast-enhanced images (D and E).

Spontaneous calyceal or renal pelvis rupture and peripelvic extravasation of urine are uncommon phenomena usually associated with ureteral obstruction from calculi [12,14]. Most cases of extravasation reported in the literature have been associated with ureteral obstruction by calculi [2,3,12,14]. Other causes include trauma and invasive urological procedures [1,2,15]. Posterior urethral valves in neonates, pregnancy and benign prostatic hypertrophy have been occasionally reported to cause urine extravasation from fornices. Rupture of the fornix or of a calyx leads to backflow of urine and contrast material into the renal sinus. Once in the renal sinus, the extravasate may enter the lymphatics (pyelolymphatic backflow) or veins (pyelovenous backflow) or may course around the pelvis into the retroperitoneum (peripelvic extravasation) [1,2,12]. In our cases with calyceal rupture, urine extravasation was demonstrated on late-phase contrast-enhanced MRI. The images were obtained 10–12 min after intravenous contrast injection. In this phase, gadolinium is excreted into the renal collecting system and is hyperintense on T1-weighted images due to its paramagnetic effect [15]. In our cases, contrast extravasation was related to calyceal rupture and was demonstrated by the hyperintense gadolinium extravasation in the perirenal and posterior pararenal spaces on T1-weighted delayed contrast-enhanced images. The T2-weighted images were sensitive to depict the smallest amount of fluid in our cases, but late contrast enhancement was necessary to show the active communication with the renal collecting system. It has been postulated that all cases of hydronephrosis have mild pyelosinus extravasation and that urine causes a local fibrotic response that prevents further disruption of the fornical area. This fact may account for the relatively few cases of peripelvic extravasation in adults with chronic

urinary tract obstruction [2,5,14,16]. This may explain the confined urinary extravasation in one of our cases with chronic hydronephrosis resulting in urinoma formation. The absence of active communication of the urinoma was demonstrated with the lack of contrast in the fluid. MRI findings of urinoma have been described in a case report previously. Urinomas may contain transudate compatible with urine or may be infected. Extravasated urine incites a low-grade inflammatory reaction followed by an avascular deposition of collagen and fibrous tissue accounting for the urinoma formation [17,18].

In conclusion, we described the spectrum of MRI findings of renal-related perinephric fluid collections. Perinephric fluid collections of pus, hemorrhage, urine and cystic fluid revealed unique imaging characteristics on noncontrast T1-weighted and T2-weighted images. The renal relation of the fluid collections was demonstrated in cases of active communication on delayed contrast-enhanced images with the contrast extravasation.

References

[1] Haddad MC, Hawary MM, Khoury NJ, Faysal SA-F, Ammouri NF, Al-Kutoubi OA. Radiology of perinephric fluid collections. Clin Radiol 2002;57:339–46.
[2] Albi G, Del Campo D, Tagarro D. Wünderlich syndrome: causes, diagnosis and radiological management. Clin Radiol 2002;57:840–5.
[3] Negus S, Sidhu S. MRI of retroperitoneal collections: a comparison with CT. Br J Radiol 2000;73:907–12.
[4] Korobkin M, Silverman PM, Quint LE, Francis IR. CT of the extraperitoneal space: normal anatomy and fluid collections. AJR Am J Roentgenol 1992;159:933–42.
[5] Unger CE, Glazer HS, Lee JKT, Ling D. MRI of extracranial hematomas: preliminary observations. AJR Am J Roentgenol 1986; 146:403–7.
[6] Chang S-Y, Ma C-P, Lee S-K. Spontaneous retroperitoneal hemorrhage from kidney causes. Eur Urol 1988;15:281–4.
[7] Balci NC, Semelka RC, Noone TC, Ascher SM. Acute and subacute liver-related hemorrhage: MRI findings. Magn Reson Imaging 1999;17:207–11.
[8] Rubin JI, Gomori JM, Grossman RI, Geffer WB, Kressel HY. High-field MR imaging of extracranial hematomas. AJR Am J Roentgenol 1987;148:813–7.
[9] Lim JH, Kim B, Auh YH. Anatomical communications of the perirenal space. Br J Radiol 1998;71:450–6.
[10] Marcos HB, Noone TC, Semelka RC. MRI evaluation of acute renal trauma. J Magn Reson Imaging 1998;8:989–90.
[11] Balci NC, Sirvanci M, Tufek I, Onat L, Duran C. Spontaneous retroperitoneal hemorrhage secondary to subcapsular renal hematoma: MRI findings. Magn Reson Imaging 2001;19:1145–8.
[12] Akpinar H, Kural AR, Tufek I, Obek C, Demirkesen O, Solok V, et al. Spontaneous ureteral rupture: is immediate surgical intervention always necessary? Presentation of four cases and review of the literature. J Endourol 2002;16:179–83.
[13] Manabe Y, Yoshioka K, Yanada J. Spontaneous rupture of a dissection of the left ovarian artery. J Med Invest 2002;49:182–5.
[14] Genes DM, Vachon L. Ultrasound finding of peripelvic urine extravasation in ureteropelvic junction obstruction. Pediatr Radiol 1989;20:122–3.
[15] Nolte-Ernsting CC, Staatz G, Tacke J, Gunther RW. MR urography today. Abdom Imaging 2003;28:191–209.
[16] Ulreich S, Lund DA, Jacobson JJ. Spontaneous rupture of a calyceal diverticulum during urography. AJR Am J Roentgenol 1978;131: 337–8.
[17] Titton RL, Gervais DA, Hahn PF, Harisinghani MG, Arellano RS, Mueller PR. Urine leaks and urinomas: diagnosis and imaging-guided intervention. Radiographics 2003;23:1133–47.
[18] Hutcheson JC, Canning DA, Hubbard AM, Johnson MP, Carr MC. Magnetic resonance imaging of fetal urinoma. Urology 2002;60:697.